Hydrol. Earth Syst. Sci. Discuss., https://doi.org/10.5194/hess-2017-599
Manuscript under review for journal Hydrol. Earth Syst. Sci.
Discussion started: 24 October 2017

Hydrology and Earth System Sciences
Open Access
Discussions

Comparison of MODIS and SWAT Evapotranspiration over a Complex Terrain at Different Spatial Scales

Olanrewaju O Abiodun[1], Huade Guan[1], Vincent E.A. Post[1], Okke Batelaan[1]

[1]National Centre for Groundwater Research and Training, College of Science and Engineering, Flinders University, Australia

Correspondence to: Olanrewaju O Abiodun (lanre.abiodun@flinders.edu.au)

Abstract. In most hydrological systems, evapotranspiration (ET) and precipitation are the largest components of the water balance, which are difficult to estimate, particularly over complex terrain. In recent decades, the advent of remotely-sensed data based ET algorithms and distributed hydrological models has provided improved spatially-upscaled ET estimates. However, information on the performance of these methods at various spatial scales is limited. This study compares the ET from the MODIS remotely sensed ET dataset (MOD16) with the ET estimates from a SWAT hydrological model for the complex terrain of the Sixth Creek Catchment of the Western Mount Lofty Ranges, South Australia. The SWAT model analyses are performed on daily timescales with a 6-year calibration period (2000-2005) and 7-year validation period (2007-2013). Differences in ET estimation between the two methods of up to 48%, 21% and 16% were observed at respectively 1 km^2, 5 km^2 and 10 km^2 spatial resolutions. Land cover differences, mismatches between the two methods and catchment-scale averaging of input climate data in the SWAT semi-distributed model were identified as the principal sources of weaker correlations at higher spatial resolution.

Key words: Evapotranspiration, MOD16, SWAT, complex terrain, spatial scale

Hydrol. Earth Syst. Sci. Discuss., https://doi.org/10.5194/hess-2017-599
Manuscript under review for journal Hydrol. Earth Syst. Sci.
Discussion started: 24 October 2017

1 Introduction

In most hydrological systems, evapotranspiration (ET) and precipitation are the largest components of the water balance (Nachabe et al., 2005) and yet the most difficult to estimate particularly over complex terrains (Wilson and Guan, 2004). In arid and semi-arid environments ET is a significant sink of groundwater with ET often exceeding precipitation (Domingo et al., 2001;Cooper et al., 2006;Scott et al., 2008;Raz-Yaseef et al., 2012). Reliable estimation of ET is integral to environmental sustainability, conservation, biodiversity and effective water resource management (Cooper et al., 2006;Boé and Terray, 2008;Zhang et al., 2008a;Tabari et al., 2013). Moreover, ET will be one of the most severely impacted hydrological components of the water cycle as a consequence of global climate change (Goyal, 2004).

Reliable, cheap and generally accessible methods of estimating ET are essential to understand its role in catchment processes. ET is principally measured and estimated using ground based measurement tools and/or through various modelling techniques often involving remote sensing (Drexler et al., 2004;Tabari et al., 2013). Ground based measurement methods such as the Bowen Ratio Energy Balance (BREB), Eddy Covariance (EC), Large Aperture Scintillometers (LAS) and lysimeters have been regarded as the most accurate and reliable ET determination methods (Kim et al., 2012a;Rana and Katerji, 2000;Liu et al., 2013b), but they are spatially and/or temporally limited (Wilson et al., 2001;Glenn et al., 2007). Despite the relative reliability of ground based measurement methods, there are inherent uncertainties associated with the different methods, which affect the accuracy of ET measurements (Baldocchi, 2003;Brotzge and Crawford, 2003;Drexler et al., 2004;Zhang et al., 2008a). Ground based measurement methods are particularly prone to significant errors related to instrument installation (Allen et al., 2011). Mu et al. (2011) observed that multiple EC towers on a site can have uncertainties ranging between 10-30% and Liu et al. (2013a) documented uncertainty ranges of over 27% between EC and LAS measurements over the same site on an annual scale. EC towers have also been observed to encounter energy balance closure challenges (Wilson et al., 2002), while other challenges of the EC method such as inaccuracies due to complex terrains have been documented by Feigenwinter et al. (2008). Furthermore, Kalma et al. (2008), conducted a review 30 remote sensing ET modelling results relative to ground based measurements and contended that the ground based measurement methods were not incontrovertibly more reliable than the remote sensing ET modelling methods. Moreover, most of the ground based measurement methods are usually cost intensive thereby constraining measurements over large areas and thus making spatial extrapolation difficult (Moran and Jackson, 1991).

In more recent years, the spatial challenges associated with ET estimations are being eased by the increased availability of remotely-sensed data. The use of remotely-sensed input data in many surface energy balance algorithms and highly parameterized hydrological models have been extensively documented (Kalma et al., 2008;Hu et al., 2015;Zhang et al., 2016). The advances in remote sensing have seen these methods become prominent in water resource assessment studies (Sun et al., 2009;Vinukollu et al., 2011;Anderson et al., 2011;Long et al., 2014;Zhang et al., 2016).

Several hydrological models and remotely-sensed based surface energy balance models are currently used in ET simulations globally (Zhao et al., 2013;Chen et al., 2014;Larsen et al., 2016;López López et al., 2016;Webster et al., 2017). However, the relative accuracy of these models relative to one another should be extensively explored to improve our understanding of the ET estimation from these algorithms. Two of the more prominent ones will be evaluated in this study – The Soil and Water Assessment Tool (SWAT) (Neitsch et al., 2011) and the MODIS ET product (Mu et al., 2013) derived from remotely-sensed data from the Moderate Resolution Imaging Spectroradiometer (MODIS) instrument aboard the National Aeronautics and Space Administration (NASA) Aqua and Terra satellites.

The MODIS ET (MOD16) is based on the Penman-Monteith equation, while the SWAT ET algorithm also has the Penman-Monteith equation as one of the three user-selectable methods of estimating ET. In this study, the Penman-Monteith method in SWAT is used for a direct comparison with the MOD16. Moreover, the Penman-Monteith equation is regarded as one of the most reliable methods for ET estimation over various climates and regions (Allen et al., 2005;Allen et al., 2006). While both the MOD16 and SWAT ET use the Penman-Monteith equation, the methods for estimating the parameters of the equation are significantly different between them. For instance, the SWAT Penman-Monteith implementation requires wind speed data for the computation of the aerodynamic resistance, while the MOD16 Penman-Monteith variant does not require wind speed data but instead uses the Biome-BGC model (Thornton, 1998) to estimate the aerodynamic resistance. This study does not seek to evaluate the individual accuracy of either method, but rather to compare the ET results from the water balance-based hydrological model (SWAT) and the energy balance-based model (MOD16) over a complex terrain catchment. The results will be compared temporally on catchment scale and spatio-temporally on sub-catchment

84 scales to identify the effects of input data and other drivers of ET estimation in the MOD16 and SWAT ET
85 algorithms.
86
87 While the MODIS evapotranspiration has been widely studied and compared to other methods, this is much less
88 the case for SWAT ET (Table 1). Moreover, a graduated spatial scale comparison of both products is yet to be
89 documented over a complex terrain. The objectives of this study are therefore: (1) To simulate and compare the
90 results of the evapotranspiration of SWAT with MOD16 over a complex terrain at a catchment scale in a semi-
91 arid climate; (2) To compare and analyse on graduated spatial scales the correlations between the MOD16 and
92 SWAT ET over a complex terrain catchment; and (3) To determine and analyse the principal drivers of ET for
93 both methods over the study area.
94

Hydrol. Earth Syst. Sci. Discuss., https://doi.org/10.5194/hess-2017-599
Manuscript under review for journal Hydrol. Earth Syst. Sci.
Discussion started: 24 October 2017

Hydrology and Earth System Sciences
Discussions

95 **Table 1:** Literature studies of MODIS and SWAT evapotranspiration (see Table 2 for climate classification)

Study Type	Reference	Method	Climate	Land Cover Cover	Spatial & temporal extents
MOD16 vs micrometeorological methods	Ruhoff et al. (2013)	EC validation at 2 sites	Cwa, Cfa	Savanna	3 km x 3 km area, 8 day
	Liu et al. (2013a)	LAS validation at 3 sites	Dwa, Cwa	Orchards, Croplands	1 km x 1 km, annual
	Mu et al. (2011)	EC validation at 46 site	Global	Global	Various
	Kim et al. (2012b)	EC validation at 17 sites	Af, Dfb, Dwa, Cfa, Bsk, Am, ET, Aw, Dwc, Dfc, Dfd	Forest, croplands, grassland	3 km x 3 km area, 8 day, 2000-2006
	Velpuri et al. (2013)	EC validation at 60 sites	Bsk, Cfa, Csa, Csb, Dfa, Dfb, Dfc	Cropland, Forest, Woody Savanna, Grassland, Shrubland, Urban	Point scale at EC sites across the United States of America, monthly, 2001 - 2007
MOD16 vs energy balance models	Jia et al. (2012)	MOD16 validation of ETWatch system	Dwa, Cwa	Farmland, Forest, Grassland,Shrub Forest, Beach land, Bare land, Urban, Paddy field	(1 km x 1 km grid over 318,000 km^2), annual , 2002-2009
	Velpuri et al. (2013)	MOD16 vs Gridded Fluxnet ET (GFET)	Bsk, Cfa, Csa, Csb, Dfa, Dfb, Dfc	Cropland, Forest, Woody Savanna, Grassland, Shrubland, Urban	50km, monthly, over the entire United States of America
MOD16 vs hydrological models	Ruhoff et al. (2013)	MOD16 vs MGB-IPH model	Cwa, Cfa	Forest, Shrubland, Savanna, Woody Savanna, Grassland, Cropland, Urban, Barren land	(1 km x 1 km grid over 145,000 km^2), 8 day, 2001
	Velpuri et al. (2013)	MOD16 vs Water Balance ET (WBET)	Bsk, Cfa, Csa, Csb, Dfa, Dfb, Dfc	Cropland, Forest, Woody Savanna, Grassland, Shrubland, Urban	(1 km x 1 km over the entire United States of America), Annual, 2002-2009,
SWAT vs energy balance models	Gao and Long (2008)	SWAT vs SEBS, SEBAL, P-TSEB, S-TSEB	Dwb	Woodland, Grassland, Cropland	1850 km^2 , 23 June 2005 and 25 July 2005 (2 days only)

96 **Table 2:** Köppen-Geiger Climate Classification system (Kottek et al., 2006)

Main climate	Precipitation	Temperature
A – equatorial	W – desert	h – hot arid
B – arid	S – steppe	k – cold arid
C – warm temperate	f – fully humid	a – hot summer
D – snow	s – summer dry	b – warm summer
E – polar	w – winter dry	c – cool summer
	m – monsoonal	d – extremely continental
		F – polar frost
		T – polar tundra

97 e.g Cwa – Warm temperate, winter dry, hot summer

98

99 ## 2 Model Description

100 ### 2.1 SWAT Model

101 The Soil and Water Assessment Tool (SWAT) is a physically based, semi-distributed hydrological model
102 designed on the water balance concept. SWAT simulates catchment processes such as evapotranspiration, runoff,
103 crop growth, nutrient and sediment transport on basis of meteorological, soil, land cover data and operational land
104 management practices (Neitsch et al., 2011). The SWAT model has been used in hydrological modelling from
105 sub-catchment scales of under 1 km^2 (Govender and Everson, 2005) to sub-continental scales (Schuol et al., 2008).
106 The model discretises a catchment into sub-catchments and further into hydrological response units (HRU), which
107 represent unique combinations of land cover, soil type and slope. The discretisation method employed by SWAT
108 enables the model to simulate catchment processes in detail and to understand the response of unique HRU's on
109 hydrological processes. Evapotranspiration is simulated at the HRU scale. A comprehensive outline of ET
110 calculations in SWAT is included in Appendix A and Fig. 1 summarizes in a flowchart the SWAT ET algorithm.
111

Hydrol. Earth Syst. Sci. Discuss., https://doi.org/10.5194/hess-2017-599
Manuscript under review for journal Hydrol. Earth Syst. Sci.
Discussion started: 24 October 2017

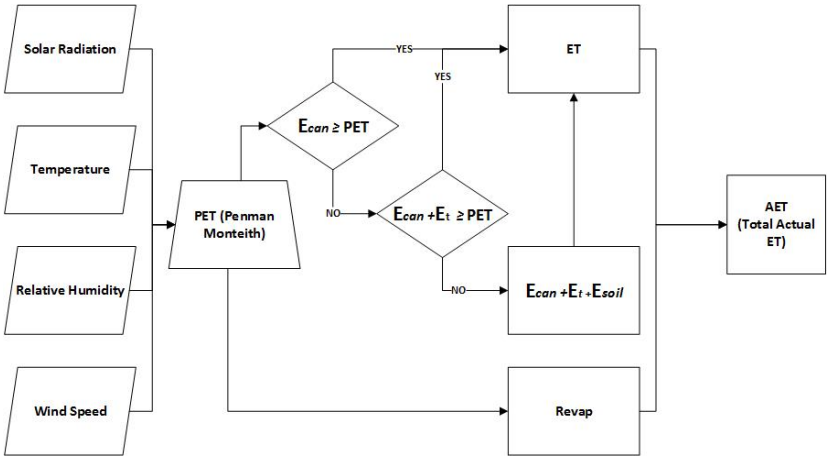

Figure 1: SWAT ET flowchart (Penman-Monteith method)

2.2 MOD16 Model

The MOD16 provides evapotranspiration estimates for 109.03×10^6 km^2 of global vegetated land area at 1 km^2 spatial resolution at 8 day, monthly and yearly temporal resolutions since the year 2000 (Mu et al., 2013). The initial version of the MOD16 algorithm used MODIS imagery as part of a Penman-Monteith method as described in Cleugh et al. (2007). The MOD16 algorithm was significantly improved by the inclusion of a sub-algorithm for estimating soil evaporation as a component of total ET (Mu et al., 2007). Further improvements on the MOD16 algorithm such as the calculation and inclusion of night time evapotranspiration, partitioning of evaporation from moist and wet soils were incorporated in the newer version of the algorithm (Mu et al., 2013). In this study, the ET products from the newer version, are used. Details of ET calculations in MOD16 are included in Appendix B while Fig. 2 summarizes in a flowchart the MOD16 ET algorithm.

Hydrol. Earth Syst. Sci. Discuss., https://doi.org/10.5194/hess-2017-599
Manuscript under review for journal Hydrol. Earth Syst. Sci.
Discussion started: 24 October 2017

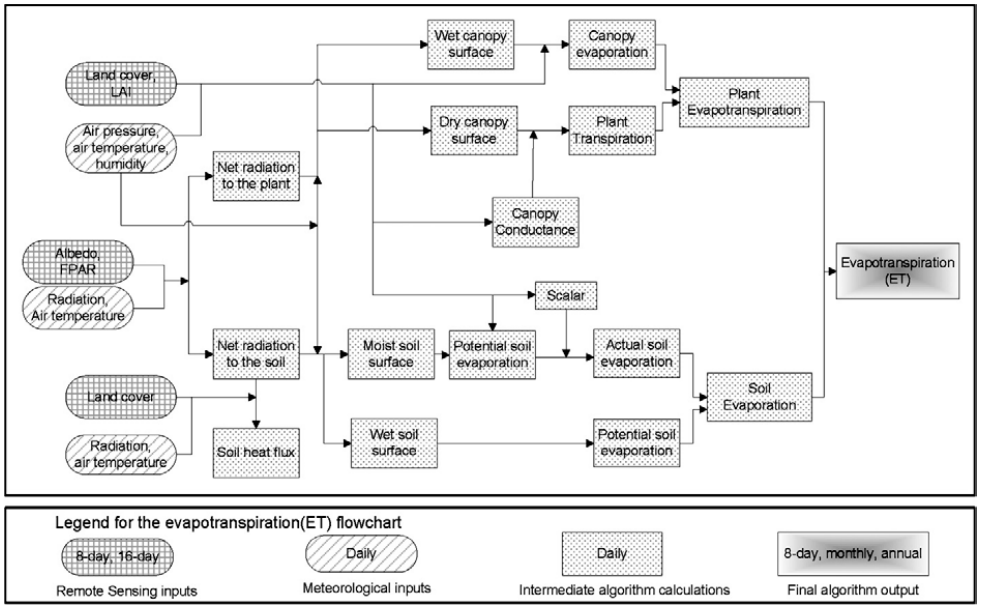

Figure 2: Flowchart of the MOD16 ET algorithm (Mu et al., 2011)

3 Data and Methods

3.1 Study Area

The study area is the Sixth Creek Catchment of South Australia, located in the western part of the Mount Lofty Ranges, which is a range of highlands separating the Adelaide Plains in the west from the Murray-Darling basin in the east. The western part of the Mount Lofty Ranges runs 90 km north to south, its summit is at 680 mAHD (metres Australian Height Datum) (Sinclair, 1980). It extends from the southernmost part at McLaren Vale on the Fleurieu Peninsula to Freeling in the north over an area of 2189 km^2. The Sixth Creek Catchment is a complex area, with acute elevation changes over few hundred metres (Fig. 3). The catchment is located close to the summit of the Western Mount Lofty Ranges.

Hydrol. Earth Syst. Sci. Discuss., https://doi.org/10.5194/hess-2017-599
Manuscript under review for journal Hydrol. Earth Syst. Sci.
Discussion started: 24 October 2017

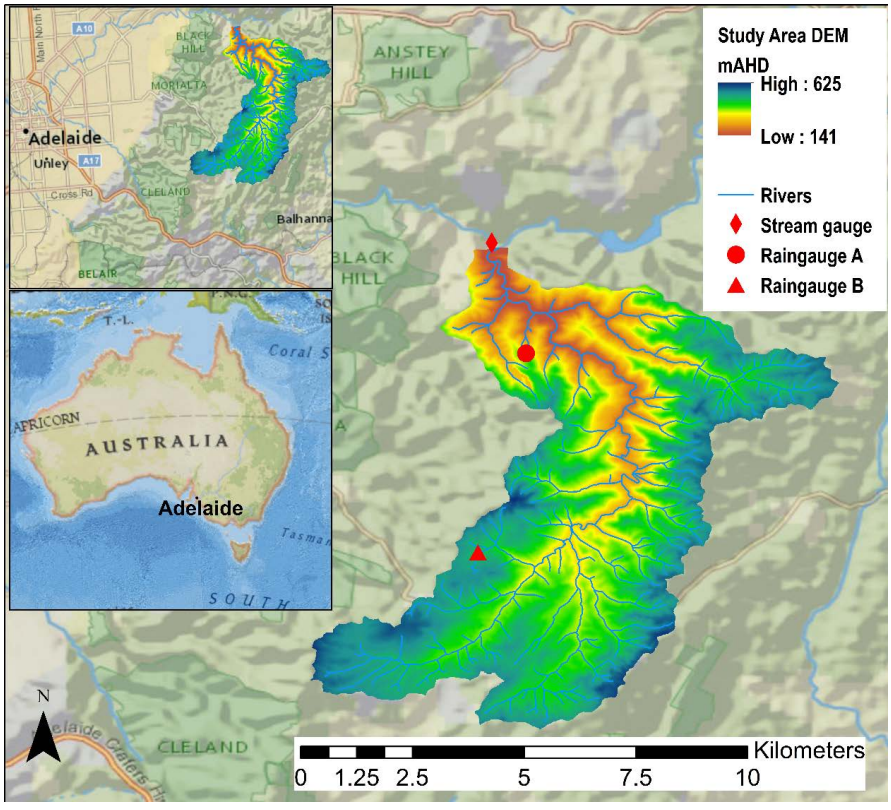

Figure 3: Digital elevation model of the Sixth Creek Catchment study area (Gallant et al., 2011),

It covers an area of 44 km^2 between 34°52′6.098″ to 34°57′54.541″S and 138°42′55.855″ to 138°49′27.174″E and has an elevation range of 140 - 625 mAHD (Fig. 3). The land cover consists of 95% forestland with significant Eucalyptus plantation and 5% pasture, shrubs and grasslands (Fig. 4b). Most of the native vegetation is under conservation. The climate is Mediterranean, with warm dry summers and cool wet winters, and is of the type "Csb" according to the Köppen-Geiger classification.

The Sixth Creek Catchment's complex terrain plays a significant role in its hydrology, with highly localised precipitation events recorded across the historic data record (2002 – 2016) from the two weather stations in the catchment. The weather stations are located 4.5 km apart with elevation difference of over 200 metres (Fig. 3). Differences in annual rainfall of over 400 mm have been recorded between the two weather stations.

Hydrol. Earth Syst. Sci. Discuss., https://doi.org/10.5194/hess-2017-599
Manuscript under review for journal Hydrol. Earth Syst. Sci.
Discussion started: 24 October 2017

The annual precipitation for the period 2002 till 2016 for Station A ranges between 500 – 900 mm and 750-1500 mm for Station B, while the temperature ranges between 10.5 °C and 22.2 °C in the summer months and 3.4 °C and 10 °C in the winter months.

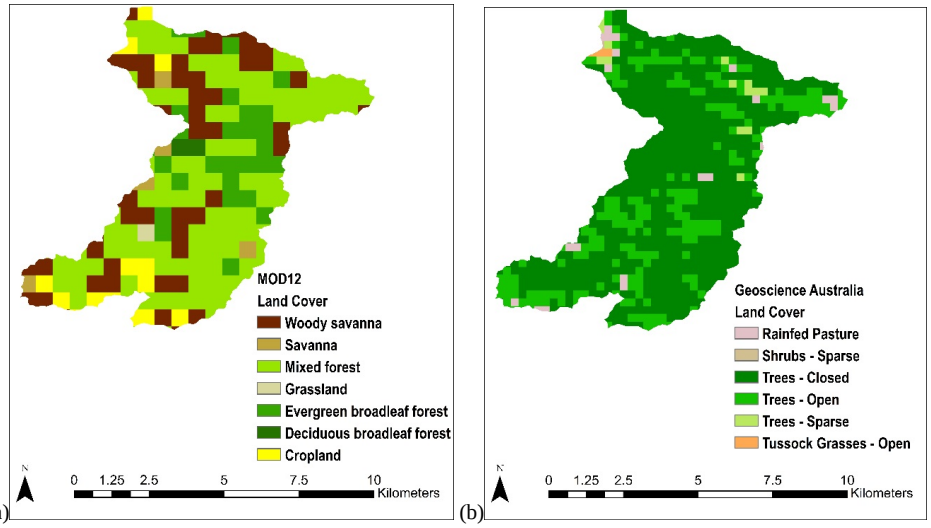

Figure 4: (a) MOD12 land cover used in MOD16 (Friedl et al., 2010); (b) Land Cover (Lymburner et al., 2010)

3.2 Input datasets

The GIS interfaced version of SWAT (ArcSWAT) was used in the hydrological modelling. A 30 m Digital Elevation Model (DEM) (Dowling et al., 2011) of the Sixth Creek Catchment was used to extract the stream network and the catchment area. A detailed soil properties database for the catchment was created from the soil data obtained from the Australian Soil Resource Information System (Johnston et al., 2003). The 250 m land cover map of Australia from Geoscience Australia's Dynamic Land Cover database (Fig. 4b) was used in the SWAT model. This land cover map was preferred to the 500 m MOD12 land cover map (Fig. 4a) due to its finer spatial resolution and better biome match with local field knowledge. In this study, the 0.01° × 0.01° wind speed data (McVicar et al., 2008), and the 0.05° × 0.05° relative humidity, temperature, rainfall, solar radiation (Jeffrey et al., 2001), were preferred to weather station data. Four 0.05° × 0.05° gridded data cells fall within the boundaries of the catchment and are therefore comparable to the climate components of the two weather stations in the catchment. Moreover, the gridded data used in this study are calibrated using the weather stations across Australia including the two weather stations in the Sixth Creek Catchment, thus maintaining excellent correlation when compared to the weather stations' measured data. Details of the gridded data methodology and algorithm used in

this study can be found in Jeffrey et al. (2001) and McVicar et al. (2008). The daily gridded climate datasets were simply averaged over the Sixth Creek Catchment, to obtain values used in this study.

The monthly MOD16 datasets for the years 2000 to 2013, at 1 km^2 spatial resolution were used in this study (Mu et al., 2013). Catchment averages were calculated by simple averaging of all the 1 km^2 cells that fall within the catchment area.

3.3 SWAT Model Setup and Calibration

The soil, land cover and DEM derived slope data were classified into classes and used to create unique HRU's. The properties of each unique HRU determine how it responds to precipitation, and how different hydrological processes such as streamflow, runoff, lateral flow and evapotranspiration are modelled in the catchment. The runoff from each HRU is accumulated and routed through the river network to the outlet of the catchment. Driven by the meteorological input, the model simulates catchment hydrological processes with a daily time step for the period 2000 to 2013.

The SWAT model is calibrated by fitting simulated streamflow to observed streamflow with the SUFI-2 algorithm. This semi-automatic Latin hypercube sampling algorithm optimizes SWAT model parameters while attempting to fit the simulated data as close as possible to the observed data using the following objective functions as measurement of simulation accuracy (Abbaspour, 2007).

Nash Sutcliffe Efficiency (N_{SE}) (Nash and Sutcliffe, 1970),

$$N_{SE} = 1 - \frac{\sum_{n=1}^{N}(Q_n - \widehat{Q_n})^2}{\sum_{n=1}^{N}(Q_n - \overline{Q})^2} \quad (1)$$

where Q_n (m^{3}s^{-1}) is the measured discharge at time n, $\widehat{Q_n}$ (m^{3}s^{-1}) is the simulated discharge at time n, $\overline{Q}$ (m^{3}s^{-1}) is the mean measured discharge and N is the number of time steps.

Ratio of root mean squared error to the standard deviation of measured data (R_{SR}) (Moriasi et al., 2007),

$$R_{SR} = \frac{\sqrt{\sum_{n=1}^{N}(Q_n - \widehat{Q_n})^2}}{\sqrt{\sum_{n=1}^{N}(Q_n - \overline{Q})^2}} \quad (2)$$

Percent bias (P_{BIAS}),

$$P_{BIAS} = 100 \ \frac{\sum_{n=1}^{N}(Q_n - \widetilde{Q_n})}{\sum_{n=1}^{N} Q_n} \quad (3)$$

Coefficient of determination (R^2),

$$R^2 = \left(\frac{(\sum_{n=1}^{N}(Q_n - \overline{Q})(\widetilde{Q_n} - \widetilde{\overline{Q_n}}))}{\sqrt{\sum_{n=1}^{N}(Q_n - \overline{Q})^2}\sqrt{\sum_{n=1}^{N}(\widetilde{Q_n} - \widetilde{Q_n})^2}} \right)^2 \quad (4)$$

where $\widetilde{Q_n}$ (m^3s^{-1}) is the mean simulated discharge.

Kling-Gupta Efficiency (K_{GE}) (Gupta et al., 2009),

$$K_{GE} = 1 - \sqrt{(r-1)^2 + (\alpha - 1)^2 + (\omega - 1)^2} \quad (5)$$

where r is the linear regression coefficient between the simulated and measured variable, $\omega = \frac{\widetilde{Q_n}}{\overline{Q}}$, $\alpha = \frac{\sigma_s}{\sigma_m}$, σ_s and σ_m are the standard deviation of simulated and measured data.

After obtaining a satisfactory fit between the simulated and observed streamflow data during calibration, the model is validated by running the model for a different time period using the same parameters from the calibration period. SUFI-2 further incorporates the P-factor and R-factor metric, which gives an indication of the confidence in the calibration exercise. The P-factor (or 95PPU) is the percentage of observed data captured which falls between the 2.5 and 97.5 percentiles (95% prediction uncertainty), while the R-factor is the width of the 95PPU. The P- and R-factors are iteratively determined using Latin Hypercube Sampling. For streamflow calibration and validation to be considered reliable, combined satisfactory values should be obtained of P-factor (> 0.7), R-factor (< 1) (Abbaspour, 2007) and of the objective functions, N_{SE} (> 0.5), R_{SR} (≤ 0.7) and P_{BIAS} (±25%) (Moriasi et al., 2007).

The calibration process was conducted on daily timescales for the years 2000 to 2005 while the validation was conducted for the years 2007 to 2013. The relatively long periods of streamflow calibration and validation on daily timescales were specifically used to address the potential problem of equifinality of parameters to be optimized. The principle of equifinality has been known to affect semi-distributed models such as SWAT (Qiao et al., 2013). Nevertheless, the use of many observation points has been observed to effectively constrain it (Tobin and Bennett, 2017). In this study, 21 sensitive SWAT model parameters (Table 3) are optimized with SUFI-2 to fit simulated streamflow to the observed streamflow data. In the SUFI-2 algorithm an “r_” and a “v_” prefix

before a SWAT model parameter indicate relative change and replacement change of the actual parameter values respectively.

The resultant SWAT simulated ET was compared with the MOD16 ET using the root mean square error (R_{MSE}), mean difference (M_D), Pearson's correlation coefficient (R) and coefficient of determination (R^2) metrics.

$$R_{MSE} = \sqrt{\frac{\sum_{n=1}^{N}(x_{1,n}-y_{1,n})}{N}} \quad (6)$$

Where x_1 and y_1 are SWAT and MOD16 monthly ET values respectively.

$$M_D = \left(\frac{x_1+x_2\ldots x_n}{n}\right) - \left(\frac{y_1+y_2\ldots y_n}{n}\right) \quad (7)$$

$$R = \frac{(\sum_{n=1}^{N}(Q_n-\overline{Q})(\widetilde{Q_n}-\widetilde{Q_n})}{\sqrt{\sum_{n=1}^{N}(Q_n-\overline{Q})^2}\sqrt{\sum_{n=1}^{N}(\widetilde{Q_n}-\widetilde{Q_n})^2}} \quad (8)$$

Hydrol. Earth Syst. Sci. Discuss., https://doi.org/10.5194/hess-2017-599
Manuscript under review for journal Hydrol. Earth Syst. Sci.
Discussion started: 24 October 2017

Hydrology and Earth System Sciences
Discussions

240 **Table 3:** Optimized SWAT parameters and their final range

Parameter Name	Parameter Description	Final Parameter Range
r_CN2.mgt	SCS Runoff Curve Number for moisture condition II	[1+ (-0.048 - 0.122)]
v_ALPHA_BF.gw	Baseflow recession constant (days)	0.58 - 0.93
v_GW_DELAY.gw	Groundwater delay time (days)	1.89 - 3.70
v_GW_REVAP.gw	Groundwater "Revap" coefficient	0.12 - 0.2
v_ESCO.hru	Soil evaporation compensation factor	0.2 - 0.5
v_CH_N2.rte	Manning's "n" value for the main channel	0.05 - 0.15
r_SURLAG.bsn	Surface runoff lag coefficient	[1+ (0.22 - 1.2)]
v_ALPHA_BNK.rte	Baseflow alpha factor for bank storage (days)	0.5 - 1
v_SOL_AWC(..sol	Available water capacity of the soil layer (mm/mm)	0.24 - 0.71
r_SOL_K(..).sol	Saturated hydraulic conductivity (mm/hr)	[1+ (-0.99 - -0.39)]
r_SOL_BD(..).sol	Moist bulk density (g/cm^3)	[1+ (-0.37 - -0.04)]
r_SOL_Z(..).sol	Depth from soil surface to bottom of layer (mm)	[1+ (-0.25 - -0.04)]
v_EPCO.bsn	Plant uptake compensation factor	0.77 – 1
v_GWQMN.gw	Threshold depth of water in the shallow aquifer required for return flow to occur (mm)	0 - 500
v_DEEPST.gw	Initial depth of water in the shallow aquifer (mm)	20000 - 30000
v_SHALLST.gw	Initial depth of water in the deep aquifer (mm)	10000 - 20000
r_HRU_SLP.hru	Average slope steepness (m/m)	[1+ (-0.24 - 0.15)]
r_OV_N.hru	Manning's "n" value for overland flow	[1+ (-0.84 - -0.05)]
r_SLSUBBSN.hru	Average slope length (m)	[1+ (-0.9 - -0.24)]
v_REVAPMN.gw	Threshold depth of water in the shallow aquifer required for Revap to occur (mm)	0 - 100
v_CH_K2.rte	Effective hydraulic conductivity in main channel alluvium (mm/hr)	6 - 30

241

242

243

Hydrol. Earth Syst. Sci. Discuss., https://doi.org/10.5194/hess-2017-599
Manuscript under review for journal Hydrol. Earth Syst. Sci.
Discussion started: 24 October 2017

Hydrology and Earth System Sciences
Discussions
Open Access
EGU

4 Results

4.1 Streamflow

The streamflow was calibrated and validated on daily timescales according to the guidelines set out in Moriasi et al. (2007) and Abbaspour (2007) (Table 4, Fig. 5). The result indicates an observed data bracketing of 89% for the calibration and 87% for the validation with both R-factors under 1.

Table 4: Streamflow calibration and validation results

	P-factor	R-factor	N_{SE}	R^2	K_{GE}	R_{SR}	P_{BIAS}
Calibration	0.89	0.66	0.61	0.62	0.71	0.62	-11.1
Validation	0.87	0.91	0.78	0.78	0.88	0.47	-0.1

Table 4 shows better results for the validation than calibration for the N_{SE}, R^2, K_{GE} and R_{SR} metrics, however slightly lower for the P-factor. The results of the calibration and validation exercise on daily timescales show that the model effectively represents the high and low flow periods (Fig. 5).

Hydrol. Earth Syst. Sci. Discuss., https://doi.org/10.5194/hess-2017-599
Manuscript under review for journal Hydrol. Earth Syst. Sci.
Discussion started: 24 October 2017

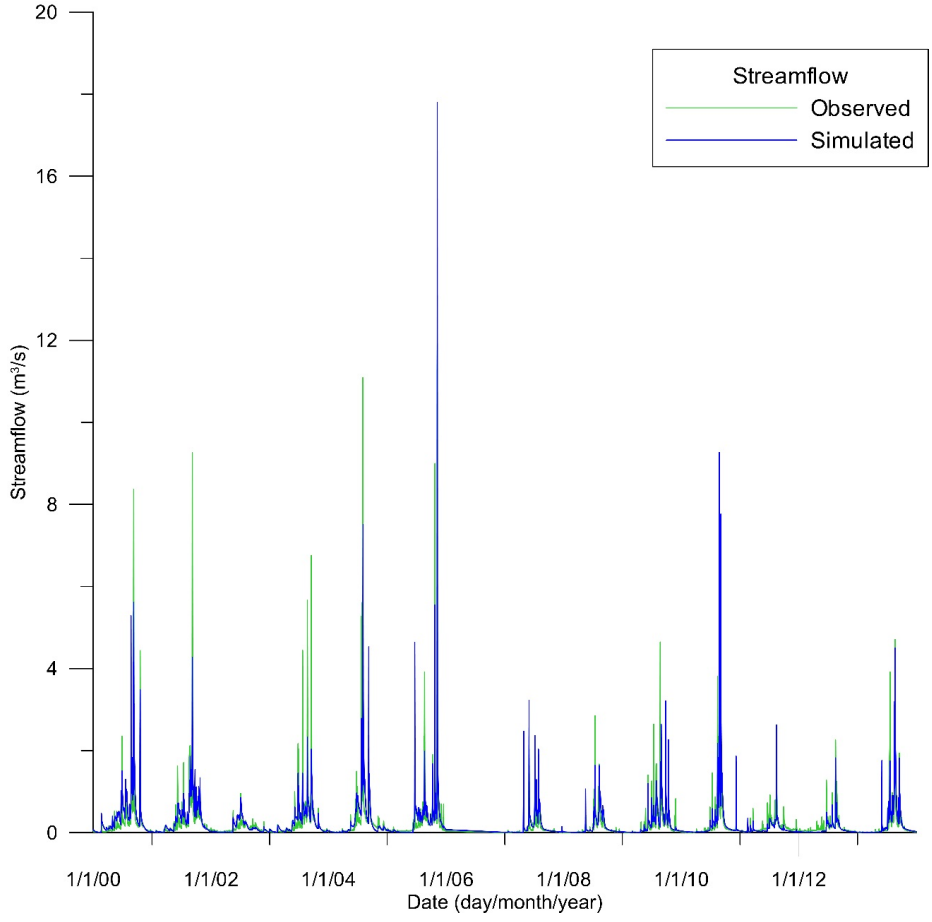

Figure 5: Streamflow calibration (2000-2005) and validation (2007-2013)

4.2 Sub-catchment scale evapotranspiration

The SWAT ET is calculated at the HRU scale (Fig. 6a), however for direct comparison with the MOD16 ET (Fig. 6c), the HRU ET results were reprocessed into 1 km^2 cells using simple averaging (Fig. 6b). Figure 6d shows the mean difference between the MOD16 and SWAT ET over the validation period at the 1 km^2 spatial resolution. The spatial distribution shows no significant correlation, except that in both datasets a trend of higher ET in the northern to central part of the catchment is seen while lower ET is observed in the south-western parts of the catchment. The spatially distributed mean annual ET difference between both methods show that about 30% of the catchment had a difference of ±100 mm/year when compared at the 1 km^2 spatial scale.

Hydrol. Earth Syst. Sci. Discuss., https://doi.org/10.5194/hess-2017-599
Manuscript under review for journal Hydrol. Earth Syst. Sci.
Discussion started: 24 October 2017

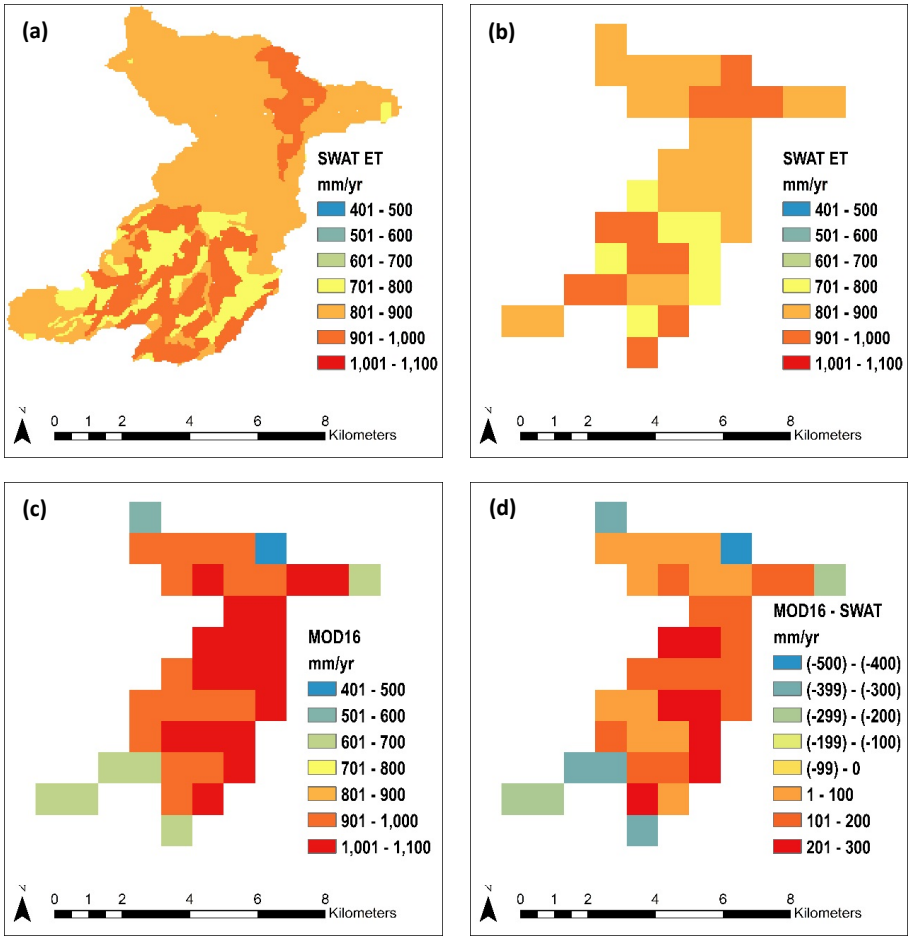

Figure 6: (a) HRU scale SWAT mean ET (2007-2013); (b) 1 km^2 grid SWAT mean ET (2007-2013); (c) 1 km^2 grid MOD16 mean ET (2007-2013); (d) Mean difference between SWAT ET and MOD16 for corresponding 1 km^2 grid cells (2007-2013)

Further analyses were carried out to determine the effect of spatial aggregation on the correspondence between the ET methods. The box and whisker plot in Fig. 7 shows the spread of the difference between the SWAT ET and the MOD16, with the bottom, middle and top of the box indicating the 25th, 50th and 75th quartiles of the distribution. The lowest and highest bars in the plot indicate the minimum and maximum differences between the ET products at the different spatial scales. On the other hand, Fig. 8 shows the minimum and maximum differences between the ET products at different spatial scales for each of the years (2007-2013). Figure 7 and 8 show that with increasing cell aggregation the difference in the ET between SWAT and MOD16 is decreasing. At 5 km^2,

Hydrol. Earth Syst. Sci. Discuss., https://doi.org/10.5194/hess-2017-599
Manuscript under review for journal Hydrol. Earth Syst. Sci.
Discussion started: 24 October 2017

the correlation was significantly higher with a maximum cell difference in ET of 21% of mean annual catchment ET compared to a maximum difference of 48% at 1 km^2 spatial resolution. At 10 km^2 spatial resolution, the maximum difference in the ET relative to the mean annual ET was 16%.

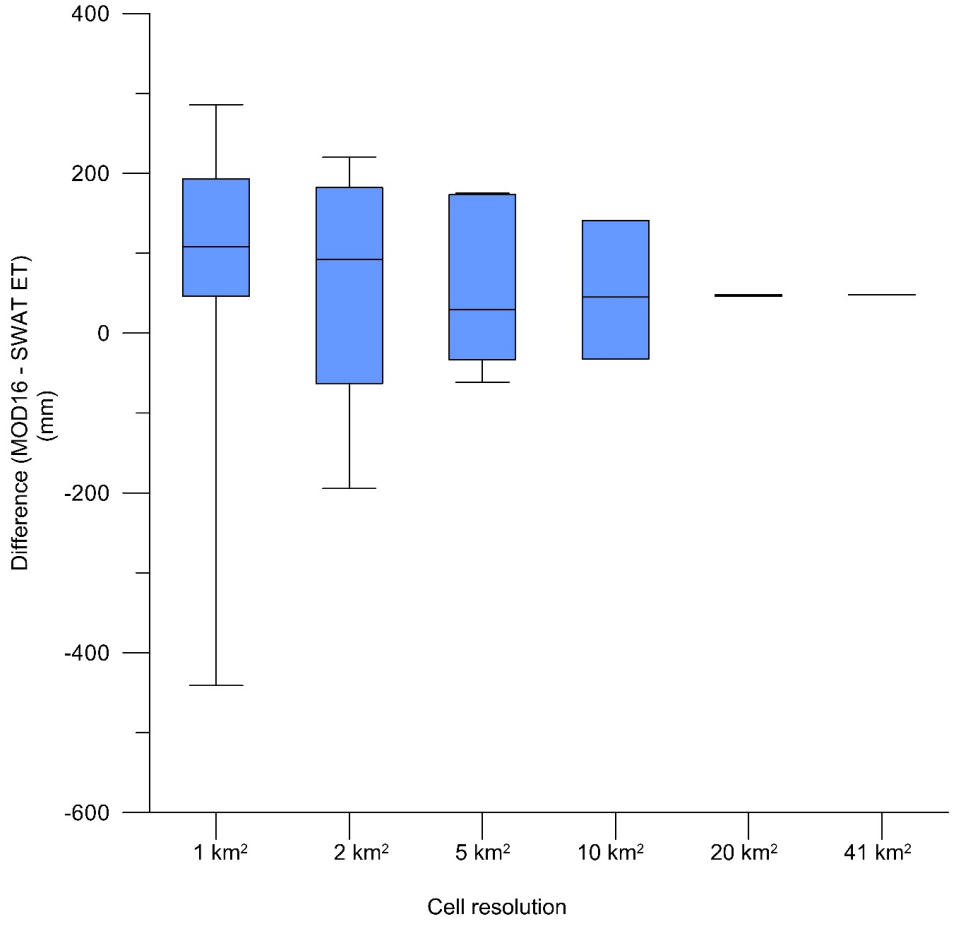

Figure 7: Differences between SWAT ET and MOD16 for cell aggregations between 1 and 41 km^2. The bottom, middle and top of the whisker indicate the 25th, 50th and 75th quartiles of the distribution, the lowest and highest bars indicate the minimum and maximum differences.

Hydrol. Earth Syst. Sci. Discuss., https://doi.org/10.5194/hess-2017-599
Manuscript under review for journal Hydrol. Earth Syst. Sci.
Discussion started: 24 October 2017

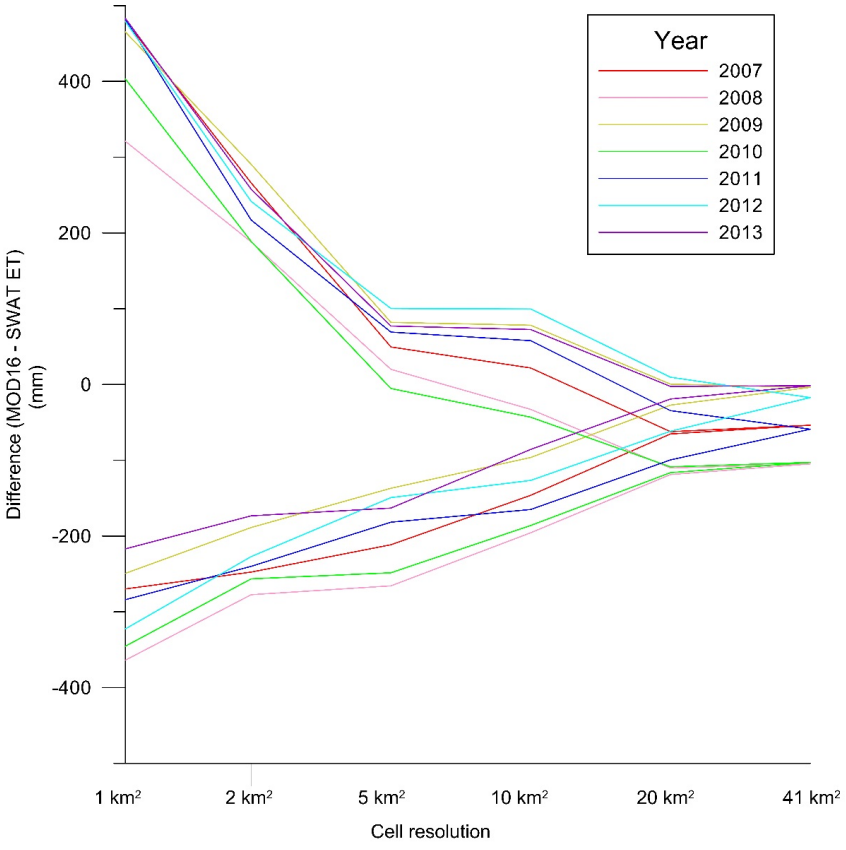

Figure 8: Minimum and maximum ET cell differences between SWAT ET and MOD16 from 2007 till 2013 at various spatial scales.

4.3 Catchment Scale Evapotranspiration

To compare the temporal dynamics, the MOD16 and the SWAT ET were also analysed at the catchment scale. Monthly MOD16 ET values at 1 km² resolution were averaged to catchment scale values using the spatial analyst tool in ArcGIS, while ET values from the validated SWAT model on catchment spatial extent and daily timescales were aggregated to monthly timescales. Using the R_{MSE}, M_D, R^2 and R metrics the analysis shows a good correspondence between the two methods at catchment scale, with a maximum annual ET difference and mean ET difference of respectively less than 13 and 6 percent for the period from 2007 to 2013 (Fig. 9).

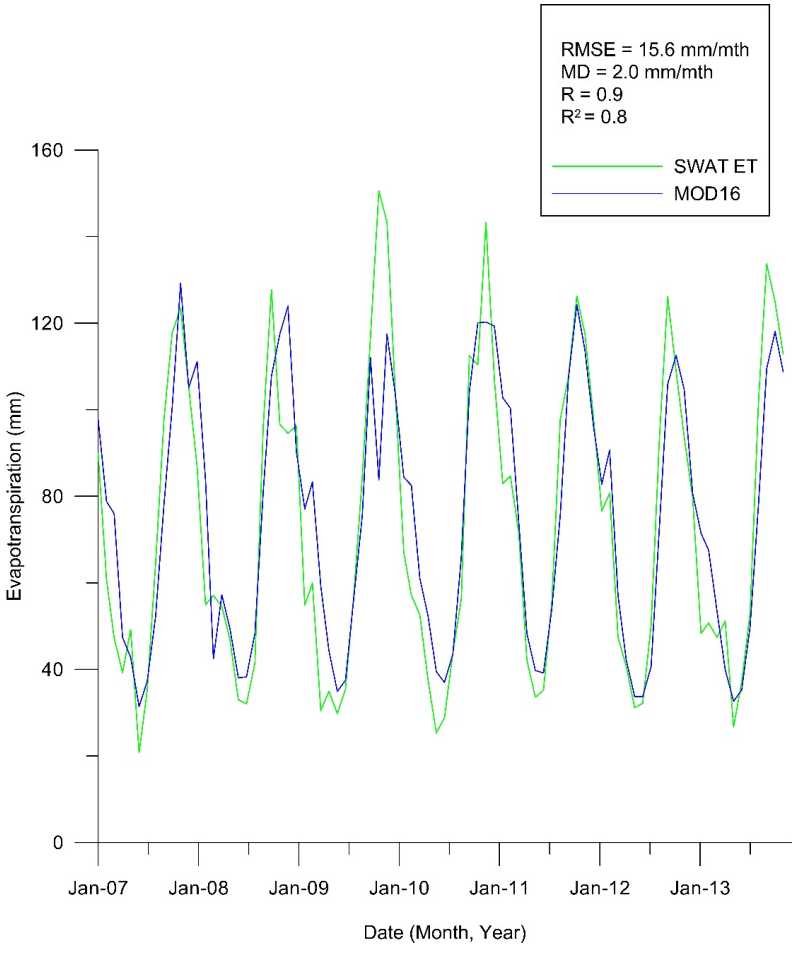

Figure 9: Monthly comparison of MOD16 and SWAT ET at catchment scale.

5 Discussion

5.1 Differences between SWAT ET and MOD16 Results

The spatial aggregation of the results of SWAT and MOD16 ET clearly exhibit weaker correlations at 1 km^2 scale compared to the catchment scale analysis. The spatial decreasing ET trend from the north-central to south-western part of the catchment shown by both methods is expected with the closed canopy forest in the north and mid-section of the catchment and a more open canopy in the southern-western parts. The recognized principal sources of differences between the ET methods are associated with land cover mismatches, biome representation, the parameterization methodology of the different components of the Penman-Monteith equation and the Revap component in SWAT; they are discussed in the following sections.

Hydrol. Earth Syst. Sci. Discuss., https://doi.org/10.5194/hess-2017-599
Manuscript under review for journal Hydrol. Earth Syst. Sci.
Discussion started: 24 October 2017

5.1.1 Land Cover

The land cover is an important parameter in the MOD16 and SWAT ET algorithms as it determines the values allocated to biophysical properties such as leaf conductance, boundary layer resistance and vapour pressure deficit (VPD), which significantly impact ET calculations. Land cover mismatches have been observed in past MOD16 studies to pose challenges in ET modeling (Mu et al., 2011;Ruhoff et al., 2013) and it is observed in this study as well. Land cover mismatches at the finer resolutions lead to weak correlation between the ET results at the 1 km^2 scale. The impact is however less significant at catchment scale. The Geoscience Land cover map has 95% percent forests, while the MOD12 has a classification of 67% forests and 24 % woody savanna, with most of the region misclassified as woody savanna having some similar properties of the forests. At catchment scale, the data averaging of the vegetation type parameters contribute to the convergence of the ET results from both methods.

5.1.2 Penman-Monteith Algorithm Parameterization

The MOD16 and SWAT ET algorithm, which are both based on the Penman-Monteith equation but parameterized differently, suggests there will be similarities and differences in the results from both methods. Both algorithms are principally limited on temporal timescales by the available energy to convert liquid water to atmospheric water vapour. Their transpiration and soil evaporation algorithms are also very dependent on vegetation/biome type, VPD, and the soil moisture constraint parameterization (Fig. 10).

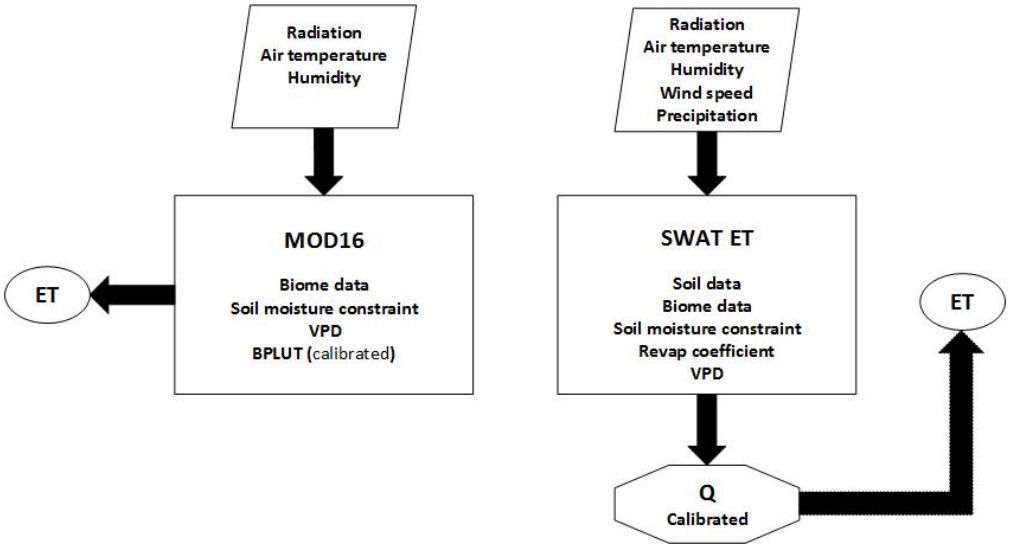

Figure 10: Major drivers of MOD16 (left) and SWAT (right) Algorithms (Q: discharge, BPLUT: biome properties lookup table; VPD: vapour pressure deficit).

330

331 In the SWAT ET algorithm, the VPD significantly impacts the transpiration through the constraining of the
332 stomatal conductance. Detailed soil data on HRU scale such as layer depth, number of layers, unsaturated
333 hydraulic conductivity and water capacity are crucial for constraining the soil moisture content, which in turn
334 regulates the percolation and recharge into the system. Similarly, the calculated MOD16 ET is significantly
335 impacted by the biome properties lookup table (BPLUT) and the soil moisture constraint function. The BPLUT
336 was calibrated using the response of biomes on flux tower sites globally. The BPLUT contains information on the
337 stomatal response of each biome to temperature, VPD and biophysical parameters. The soil moisture constraint
338 function is applied in the estimation of the soil evaporation and is an important parameter in regions where the
339 saturated zone is close to the ground surface.

340

341 The impact of the differences in the parameterization methodology are more significant at smaller spatial scales
342 due to the diverse input data and their associated errors, these impacts become less significant as the outputs are
343 up-scaled (Fig. 8). This trend was also observed by Hong et al. (2009). The convergence of the results of the two
344 methods at catchment scale is also strongly attributed to the simple averaging used in this study to aggregate the
345 ET outputs from the MOD16 and SWAT ET to catchment scales. The simple averaging method has been observed
346 to be the best in flux aggregation after a study of various methods (Ershadi et al., 2013).

347

348 **5.1.3 Revap**

349 The Revap component of the AET in SWAT is mostly significant in forested catchments with deep rooted trees
350 that can access the saturated zone and as such are governed by land use parameters (Neitsch et al., 2011). However,
351 the relative accuracy of the Revap component of the ET on HRU scales has been questioned (Liu et al., 2015) due
352 to the linear relationship between the Revap coefficient and potential evapotranspiration in SWAT (see Eqn. A23).
353 The Revap component in this study appears consistent with the studies by Benyon et al. (2006) in south-eastern
354 Australia with similar climatic condition as the Sixth Creek Catchment. Benyon et al. (2006) observed that under
355 the combined conditions of highly permeable soils, available groundwater resources of low salinity (<2000 mg/L),
356 a high transmissivity aquifer and groundwater of depths up to 6 m, annual groundwater ET contribution to total
357 ET ranged from 13 – 72% for sampled Eucalyptus tree species. The Sixth Creek Catchment is principally
358 underlain by the highly transmissive and permeable Aldgate Sandstone aquifer, with salinity levels well below
359 2000 mg/L (Gerges, 1999). Monitoring bores in the Sixth Creek Catchment have recorded standing water levels

Hydrol. Earth Syst. Sci. Discuss., https://doi.org/10.5194/hess-2017-599
Manuscript under review for journal Hydrol. Earth Syst. Sci.
Discussion started: 24 October 2017

of less than 1.5 metres at the end of the rainy winter months. The Sixth Creek Catchment has been identified as one of the principal recharge zones in the Western Mount Lofty Ranges based on the catchment geology and hydrochemical analysis (Green and Zulfic, 2008). A significant portion of the 95% forested part of the Sixth Creek Catchment is a mosaic of various Eucalyptus tree species, thereby corroborating the results of Benyon et al. (2006). The results suggest the Revap is a significant contributor to ET in the Sixth Creek Catchment (Fig. 11) with mean annual contribution of 20% for the years 2007 – 2013, while monthly contributions ranged from 15 – 52 % over the same period. The possibility exists that the linear relationship with PET employed in its calculation on HRU scale may be contributory to the higher range of ET fluctuation seen in the SWAT model on the 1 km^2 scale when compared to the MOD16, however, that is beyond the scope of this study.

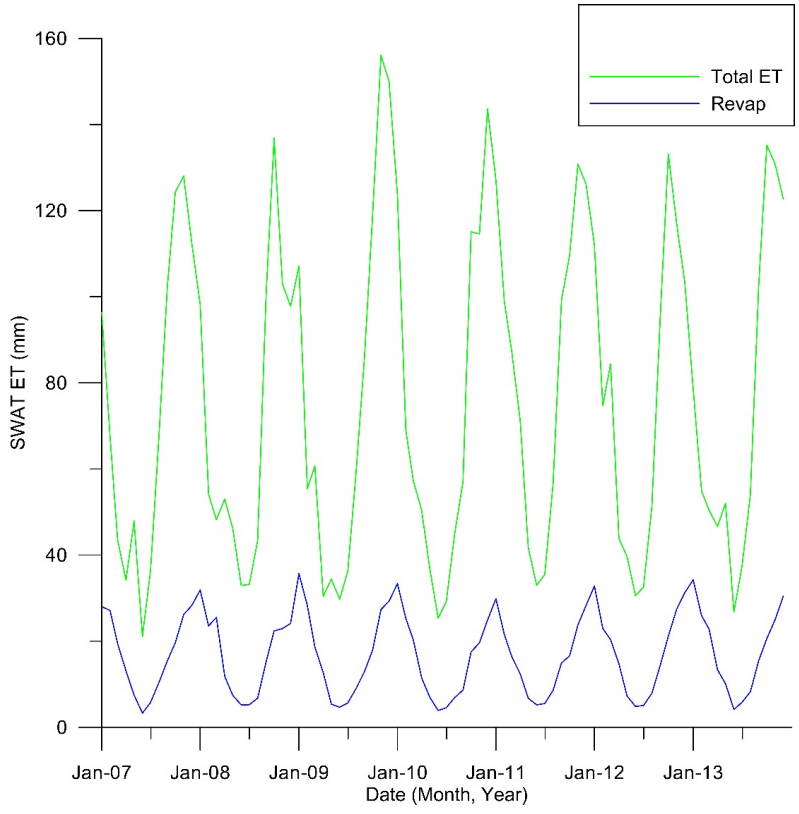

Fig 11. Monthly comparison of Revap component of the ET and total ET in SWAT.

On catchment scale, the results show that MOD16 simulates higher ET in the winter periods while SWAT simulates higher ET during the summer periods (Fig. 9). Generally, the agreement between the products is more

consistent during the winter seasons when ET is lower. The lesser correlation during higher ET seasons may be related to the linearly determined Revap component of the ET, which is a more dominant process in the summer months when the demand for soil evaporation, plant transpiration and groundwater ET is significantly higher,

5.2 Input data Challenges

The SWAT ET and the MOD16 methods both have challenges associated with input data, which are subsequently propagated through the algorithm. In semi-arid environments such as the Sixth Creek Catchment, high intensity rainfall events are common occurrences, which impacts hydrologic processes such as infiltration and evapotranspiration differently from if the precipitation were evenly distributed through the day (Syed et al., 2003). Yang et al. (2016) observed that the use of hourly rainfall in SWAT significantly improved the modelling of streamflow and hydrological processes. In this study, due to the unavailability of hourly precipitation data, daily precipitation data were used thus neglecting the impact of high intensity precipitation events in the catchment.

Another challenge encountered with the SWAT model is associated with the semi-distributed model methodology. The use of a single value for wind speed, relative humidity and solar radiation for a sub-catchment with spatial scale, which could be in the order of tens of square kilometres, affects the accuracy of hydrological processes at the HRU scale. The “elevation band” method of temperature and precipitation distribution with respect to elevation changes across a catchment was introduced into the SWAT algorithm to attenuate orographic effects in complex terrain catchments (Neitsch et al., 2011). The elevation band algorithm in SWAT has performed well in predominantly snowy, complex terrain catchments, which are significantly larger than the Sixth Creek Catchment with elevation changes in the order of kilometres (Abbaspour et al., 2007;Zhang et al., 2008b;Pradhanang et al., 2011). However, the application of the elevation band algorithm in the non-snowy Odiel River basin (Spain) with Mediterranean climate similar to the Sixth Creek Catchment yielded less than satisfactory results (Galván et al., 2014). In the non-snowy Sixth Creek Catchment, the orographic effects are a dominant atmospheric process when winds are moving from the lower elevations in the north of the catchment to the higher elevations in the South particularly during the winter months. The orographic lift leads to significantly higher precipitation in the south-westerly direction in the Sixth Creek Catchment, which the elevation band algorithm in SWAT does not represent accurately in non-snowy catchments.

403

404 The various meteorological and remote sensing input data used in the processing of the MOD16 all have their
405 inherent uncertainties, with cloud cover challenges and coarse resolution resampling (Mu et al., 2011), while
406 errors have been associated with the land cover product used (Ruhoff et al., 2013). The land cover map
407 (MOD12) used in MOD16 (Fig. 4a), in conjunction with the calibrated biome properties lookup table (BPLUT)
408 significantly influences the ET output from the various land covers under different climatic conditions. A more
409 detailed map and local knowledge of the Sixth Creek Catchment indicates that the MOD12 land cover spatially
410 mismatches some biomes (Fig. 4a and 4b). Besides the obvious land cover mismatches that were observed
411 between the input data of the two models, the variety of accepted national, regional and global land cover
412 classification system contributes to the challenges of hydrological modelling. In this MOD12, the “mixed
413 forest” category covered over 50% of the catchment while the category does not exist in the local field map land
414 cover classification. The global standardization and harmonization of land cover maps and biome classification
415 at high resolution may improve model performance.

416

417 **6 Conclusion**

418 The main objectives of this paper are to compare the ET results from a streamflow calibrated SWAT model and
419 the MOD16 in a complex terrain catchment, to analyse the graduated spatial correlations between MOD16 and
420 SWAT ET and also evaluate the drivers of the ET algorithm in both models.

421

422 The calibrated SWAT model using the SUFI-2 algorithm and various objective functions could simulate ET to
423 within 6% of the MOD16 on catchment scale, annually. The P and R factors metrics were observed to be very
424 reliable indicators of a good calibration exercise. Abbaspour (2007) proposed P and R factor minimum
425 benchmarks of >0.7 and <1 respectively for streamflow calibration, in this study the P and R factors >0.8 and <1
426 were found to produce reliable ET estimates on catchment scales.

427

428 Both models show good correlation on catchment scale while biome differences and input spatial scale differences
429 are responsible for weak correlation at finer spatial scales. The challenge of the lack of a globally accepted and
430 harmonised land cover classification system at high resolution was encountered in the study, with two products
431 derived from the MODIS satellite data classifying land cover differently and thus impacting the results from both
432 models. The use of different land covers with different classification systems and parameters have limited impact

433 on evapotranspiration modelling at coarse spatial resolutions due to spatial averaging. This is not the case at finer
434 spatial resolutions where the impact of each land cover parameter is prominent. The inherent differences and
435 uncertainties associated with these land cover products will continue to be propagated through the models, thereby
436 promoting divergence in the drive towards more accurate and finer resolution evapotranspiration data products.
437 While many concerted research efforts have been made in the past (Latham, 2009;Friedl et al., 2010), a globally
438 accepted harmonised world land cover database at high resolution can significantly improve correlation and
439 confidence in high resolution ET products.
440
441 The result of the spatial resolution analysis corroborates the view that prevailing ET algorithms and measurement
442 methods will have certain degree of variability due to the complexity of ET estimation and various drivers of the
443 contributory processes. The study shows that correlation at catchment scale does not necessarily translate to
444 correlation at finer spatial scales. The study also highlights the possible challenges of the semi-distributed SWAT
445 ET algorithm in a complex terrain as the input climate data can be a challenge due to spatial resolution and climate
446 variability.
447
448

References

Abbaspour, K.: User manual for SWAT-CUP, SWAT calibration and uncertainty analysis programs, Swiss Federal Institute of Aquatic Science and Technology, Eawag, Duebendorf, Switzerland, 2007.

Abbaspour, K. C., Yang, J., Maximov, I., Siber, R., Bogner, K., Mieleitner, J., Zobrist, J., and Srinivasan, R.: Modelling hydrology and water quality in the pre-alpine/alpine Thur watershed using SWAT, Journal of hydrology, 333, 413-430, 2007.

Allen, R. G., Clemmens, A. J., Burt, C. M., Solomon, K., and O'Halloran, T.: Prediction accuracy for projectwide evapotranspiration using crop coefficients and reference evapotranspiration, Journal of Irrigation and Drainage Engineering, 131, 24-36, 2005.

Allen, R. G., Pruitt, W. O., Wright, J. L., Howell, T. A., Ventura, F., Snyder, R., Itenfisu, D., Steduto, P., Berengena, J., and Yrisarry, J. B.: A recommendation on standardized surface resistance for hourly calculation of reference ET o by the FAO56 Penman-Monteith method, Agricultural Water Management, 81, 1-22, 2006.

Allen, R. G., Pereira, L. S., Howell, T. A., and Jensen, M. E.: Evapotranspiration information reporting: I. Factors governing measurement accuracy, Agr Water Manage, 98, 899-920, 2011.

Anderson, M. C., Hain, C., Wardlow, B., Pimstein, A., Mecikalski, J. R., and Kustas, W. P.: Evaluation of drought indices based on thermal remote sensing of evapotranspiration over the continental United States, Journal of Climate, 24, 2025-2044, 2011.

Baldocchi, D. D.: Assessing the eddy covariance technique for evaluating carbon dioxide exchange rates of ecosystems: past, present and future, Global Change Biology, 9, 479-492, 2003.

Benyon, R. G., Theiveyanathan, S., and Doody, T. M.: Impacts of tree plantations on groundwater in south-eastern Australia, Australian Journal of Botany, 54, 181-192, 2006.

Boé, J., and Terray, L.: Uncertainties in summer evapotranspiration changes over Europe and implications for regional climate change, Geophysical Research Letters, 35, 2008.

Brotzge, J. A., and Crawford, K. C.: Examination of the surface energy budget: A comparison of eddy correlation and Bowen ratio measurement systems, Journal of Hydrometeorology, 4, 160-178, 2003.

Chen, Y., Xia, J., Liang, S., Feng, J., Fisher, J. B., Li, X., Li, X., Liu, S., Ma, Z., and Miyata, A.: Comparison of satellite-based evapotranspiration models over terrestrial ecosystems in China, Remote sensing of environment, 140, 279-293, 2014.

Cleugh, H. A., Leuning, R., Mu, Q., and Running, S. W.: Regional evaporation estimates from flux tower and MODIS satellite data, Remote Sensing of Environment, 106, 285-304, 2007.

Cooper, D. J., Sanderson, J. S., Stannard, D. I., and Groeneveld, D. P.: Effects of long-term water table drawdown on evapotranspiration and vegetation in an arid region phreatophyte community, Journal of Hydrology, 325, 21-34, 2006.

Domingo, F., Villagarcıa, L., Boer, M., Alados-Arboledas, L., and Puigdefábregas, J.: Evaluating the long-term water balance of arid zone stream bed vegetation using evapotranspiration modelling and hillslope runoff measurements, Journal of Hydrology, 243, 17-30, 2001.

Dowling, T., Brooks, M., and Read, A.: Continental hydrologic assessment using the 1 second (30m) resolution Shuttle Radar Topographic Mission DEM of Australia, 19th International Congress on Modelling and Simulation. Perth, 2011,

Drexler, J. Z., Snyder, R. L., Spano, D., Paw, U., and Tha, K.: A review of models and micrometeorological methods used to estimate wetland evapotranspiration, Hydrological Processes, 18, 2071-2101, 2004.

Ershadi, A., McCabe, M., Evans, J. P., and Walker, J. P.: Effects of spatial aggregation on the multi-scale estimation of evapotranspiration, Remote Sensing of Environment, 131, 51-62, 2013.

Feigenwinter, C., Bernhofer, C., Eichelmann, U., Heinesch, B., Hertel, M., Janous, D., Kolle, O., Lagergren, F., Lindroth, A., and Minerbi, S.: Comparison of horizontal and vertical advective CO 2 fluxes at three forest sites, agricultural and forest meteorology, 148, 12-24, 2008.

Fisher, J. B., Tu, K. P., and Baldocchi, D. D.: Global estimates of the land–atmosphere water flux based on monthly AVHRR and ISLSCP-II data, validated at 16 FLUXNET sites, Remote Sensing of Environment, 112, 901-919, 2008.

499 Friedl, M. A., Sulla-Menashe, D., Tan, B., Schneider, A., Ramankutty, N., Sibley, A., and Huang, X.:
500 MODIS Collection 5 global land cover: Algorithm refinements and characterization of new datasets,
501 Remote Sens Environ, 114, 168-182, 2010.
502 Galván, L., Olías, M., Izquierdo, T., Cerón, J., and de Villarán, R. F.: Rainfall estimation in SWAT: An
503 alternative method to simulate orographic precipitation, Journal of hydrology, 509, 257-265, 2014.
504 Gao, Y., and Long, D.: Intercomparison of remote sensing-based models for estimation of
505 evapotranspiration and accuracy assessment based on SWAT, Hydrological processes, 22, 4850-4869,
506 2008.
507 Gerges, N. Z.: The Geology & Hydrogeology of the Adelaide Metropolitan Area, PhD thesis, Faculty of
508 Science and Engineering, Flinders University of South Australia, Adelaide, SA, 1999.
509 Glenn, E. P., Huete, A. R., Nagler, P. L., Hirschboeck, K. K., and Brown, P.: Integrating remote sensing
510 and ground methods to estimate evapotranspiration, Critical Reviews in Plant Sciences, 26, 139-168,
511 2007.
512 Govender, M., and Everson, C.: Modelling streamflow from two small South African experimental
513 catchments using the SWAT model, Hydrological Processes, 19, 683-692, 2005.
514 Goyal, R.: Sensitivity of evapotranspiration to global warming: a case study of arid zone of Rajasthan
515 (India), Agr Water Manage, 69, 1-11, 2004.
516 Green, G., and Zulfic, D.: Summary of groundwater recharge estimates for the catchments of the
517 Western Mount Lofty Ranges Prescribed Water Resources Area, Department of Water, Land and
518 Biodiversity Conservation, 2008.
519 Gupta, H. V., Kling, H., Yilmaz, K. K., and Martinez, G. F.: Decomposition of the mean squared error and
520 NSE performance criteria: Implications for improving hydrological modelling, Journal of Hydrology,
521 377, 80-91, 2009.
522 Hong, S.-h., Hendrickx, J. M., and Borchers, B.: Up-scaling of SEBAL derived evapotranspiration maps
523 from Landsat (30m) to MODIS (250m) scale, Journal of hydrology, 370, 122-138, 2009.
524 Hu, G., Jia, L., and Menenti, M.: Comparison of MOD16 and LSA-SAF MSG evapotranspiration products
525 over Europe for 2011, Remote Sensing of Environment, 156, 510-526, 2015.
526 Jeffrey, S. J., Carter, J. O., Moodie, K. B., and Beswick, A. R.: Using spatial interpolation to construct a
527 comprehensive archive of Australian climate data, Environmental Modelling & Software, 16, 309-330,
528 http://dx.doi.org/10.1016/S1364-8152(01)00008-1, 2001.
529 Jensen, M. E., Burman, R. D., and Allen, R. G.: Evapotranspiration and irrigation water requirements,
530 1990,
531 Jia, Z., Liu, S., Xu, Z., Chen, Y., and Zhu, M.: Validation of remotely sensed evapotranspiration over the
532 Hai River Basin, China, Journal of Geophysical Research: Atmospheres, 117, n/a-n/a,
533 10.1029/2011JD017037, 2012.
534 Johnston, R., Barry, S., Bleys, E., Bui, E. N., Moran, C., Simon, D., Carlile, P., McKenzie, N., Henderson,
535 B., and Chapman, G.: ASRIS: the database, Soil Research, 41, 1021-1036, 2003.
536 Kalma, J. D., McVicar, T. R., and McCabe, M. F.: Estimating land surface evaporation: A review of
537 methods using remotely sensed surface temperature data, Surveys in Geophysics, 29, 421-469, 2008.
538 Kim, H., Hwang, K., Mu, Q., Lee, S., and Choi, M.: Validation of MODIS 16 global terrestrial
539 evapotranspiration products in various climates and land cover types in Asia, KSCE Journal of Civil
540 Engineering, 16, 229-238, 10.1007/s12205-012-0006-1, 2012a.
541 Kim, H. W., Hwang, K., Mu, Q., Lee, S. O., and Choi, M.: Validation of MODIS 16 global terrestrial
542 evapotranspiration products in various climates and land cover types in Asia, KSCE Journal of Civil
543 Engineering, 16, 229-238, 2012b.
544 Kottek, M., Grieser, J., Beck, C., Rudolf, B., and Rubel, F.: World map of the Köppen-Geiger climate
545 classification updated, Meteorologische Zeitschrift, 15, 259-263, 2006.
546 Larsen, M. A., Refsgaard, J. C., Jensen, K. H., Butts, M. B., Stisen, S., and Mollerup, M.: Calibration of a
547 distributed hydrology and land surface model using energy flux measurements, Agricultural and Forest
548 Meteorology, 217, 74-88, 2016.
549 Latham, J.: FAO land cover mapping initiatives, North America Land Cover Summit, 75-95, 2009.

Liu, S., Xu, Z., Zhu, Z., Jia, Z., and Zhu, M.: Measurements of evapotranspiration from eddy-covariance systems and large aperture scintillometers in the Hai River Basin, China, Journal of hydrology, 487, 24-38, 2013a.

Liu, S. M., Xu, Z. W., Zhu, Z. L., Jia, Z. Z., and Zhu, M. J.: Measurements of evapotranspiration from eddy-covariance systems and large aperture scintillometers in the Hai River Basin, China, Journal of Hydrology, 487, 24-38, http://dx.doi.org/10.1016/j.jhydrol.2013.02.025, 2013b.

Liu, T., Liu, L., Luo, Y., and Lai, J.: Simulation of groundwater evaporation and groundwater depth using SWAT in the irrigation district with shallow water table, Environmental Earth Sciences, 74, 315-324, 2015.

Long, D., Longuevergne, L., and Scanlon, B. R.: Uncertainty in evapotranspiration from land surface modeling, remote sensing, and GRACE satellites, Water Resources Research, 50, 1131-1151, 2014.

López López, P., Strohmeier, S., Haddad, M., Sutanudjaja, E., Karrou, M., Sterk, G., Schellekens, J., and Bierkens, M.: Application of earth observation products for hydrological modeling of the Oum Er Rbia river basin, EGU General Assembly Conference Abstracts, 2016, 12117,

Lymburner, L., Tan, P., Mueller, N., Thackway, R., Lewis, A., Thankappan, M., Randall, L., Islam, A., and Senarath, U.: 250 metre dynamic land cover dataset of Australia, Geoscience Australia, Canberra, 2010.

McVicar, T. R., Van Niel, T. G., Li, L. T., Roderick, M. L., Rayner, D. P., Ricciardulli, L., and Donohue, R. J.: Wind speed climatology and trends for Australia, 1975–2006: Capturing the stilling phenomenon and comparison with near-surface reanalysis output, Geophysical Research Letters, 35, n/a-n/a, 10.1029/2008GL035627, 2008.

Moran, M. S., and Jackson, R. D.: Assessing the spatial distribution of evapotranspiration using remotely sensed inputs, J Environ Qual, 20, 725-737, 1991.

Moriasi, D. N., Arnold, J. G., Van Liew, M. W., Bingner, R. L., Harmel, R. D., and Veith, T. L.: Model evaluation guidelines for systematic quantification of accuracy in watershed simulations, T Asabe, 50, 885-900, 2007.

Mu, Q., Heinsch, F. A., Zhao, M., and Running, S. W.: Development of a global evapotranspiration algorithm based on MODIS and global meteorology data, Remote Sensing of Environment, 111, 519-536, DOI 10.1016/j.rse.2007.04.015, 2007.

Mu, Q., Zhao, M., and Running, S. W.: Improvements to a MODIS global terrestrial evapotranspiration algorithm, Remote Sensing of Environment, 115, 1781-1800, http://dx.doi.org/10.1016/j.rse.2011.02.019, 2011.

Mu, Q., Zhao, M., and Running, S. W.: MODIS Global Terrestrial Evapotranspiration (ET) Product (NASA MOD16A2/A3), Algorithm Theoretical Basis Document, Collection, 5, 2013.

Nachabe, M., Shah, N., Ross, M., and Vomacka, J.: Evapotranspiration of two vegetation covers in a shallow water table environment, Soil Sci Soc Am J, 69, 492-499, 2005.

Nash, J. E., and Sutcliffe, J. V.: River flow forecasting through conceptual models part I—A discussion of principles, Journal of hydrology, 10, 282-290, 1970.

Neitsch, S. L., Arnold, J. G., Kiniry, J. R., and Williams, J. R.: Soil and water assessment tool theoretical documentation version 2009, Texas Water Resources Institute, 2011.

Pradhanang, S. M., Anandhi, A., Mukundan, R., Zion, M. S., Pierson, D. C., Schneiderman, E. M., Matonse, A., and Frei, A.: Application of SWAT model to assess snowpack development and streamflow in the Cannonsville watershed, New York, USA, Hydrological Processes, 25, 3268-3277, 2011.

Qiao, L., Herrmann, R. B., and Pan, Z.: Parameter uncertainty reduction for SWAT using GRACE, streamflow, and groundwater table data for Lower Missouri River Basin, JAWRA Journal of the American Water Resources Association, 49, 343-358, 2013.

Rana, G., and Katerji, N.: Measurement and estimation of actual evapotranspiration in the field under Mediterranean climate: a review, European Journal of agronomy, 13, 125-153, 2000.

599 Raz-Yaseef, N., Yakir, D., Schiller, G., and Cohen, S.: Dynamics of evapotranspiration partitioning in a
600 semi-arid forest as affected by temporal rainfall patterns, Agricultural and Forest Meteorology, 157,
601 77-85, 2012.
602 Ruhoff, A. L., Paz, A. R., Aragao, L. E. O. C., Mu, Q., Malhi, Y., Collischonn, W., Rocha, H. R., and Running,
603 S. W.: Assessment of the MODIS global evapotranspiration algorithm using eddy covariance
604 measurements and hydrological modelling in the Rio Grande basin, Hydrological Sciences Journal, 58,
605 1658-1676, 10.1080/02626667.2013.837578, 2013.
606 Schuol, J., Abbaspour, K. C., Srinivasan, R., and Yang, H.: Estimation of freshwater availability in the
607 West African sub-continent using the SWAT hydrologic model, Journal of Hydrology, 352, 30-49, 2008.
608 Scott, R. L., Cable, W. L., Huxman, T. E., Nagler, P. L., Hernandez, M., and Goodrich, D. C.: Multiyear
609 riparian evapotranspiration and groundwater use for a semiarid watershed, Journal of Arid
610 Environments, 72, 1232-1246, 2008.
611 Sun, Z., Wang, Q., Matsushita, B., Fukushima, T., Ouyang, Z., and Watanabe, M.: Development of a
612 simple remote sensing evapotranspiration model (Sim-ReSET): algorithm and model test, Journal of
613 Hydrology, 376, 476-485, 2009.
614 Syed, K. H., Goodrich, D. C., Myers, D. E., and Sorooshian, S.: Spatial characteristics of thunderstorm
615 rainfall fields and their relation to runoff, Journal of hydrology, 271, 1-21, 2003.
616 Tabari, H., Grismer, M. E., and Trajkovic, S.: Comparative analysis of 31 reference evapotranspiration
617 methods under humid conditions, Irrigation Science, 31, 107-117, 2013.
618 Thornton, P. E.: Regional ecosystem simulation: Combining surface-and satellite-based observations
619 to study linkages between terrestrial energy and mass budgets, 1998.
620 Tobin, K. J., and Bennett, M. E.: Constraining SWAT Calibration with Remotely Sensed
621 Evapotranspiration Data, JAWRA Journal of the American Water Resources Association, 53, 593-604,
622 2017.
623 Velpuri, N. M., Senay, G. B., Singh, R. K., Bohms, S., and Verdin, J. P.: A comprehensive evaluation of
624 two MODIS evapotranspiration products over the conterminous United States: Using point and
625 gridded FLUXNET and water balance ET, Remote Sensing of Environment, 139, 35-49, 2013.
626 Vinukollu, R. K., Wood, E. F., Ferguson, C. R., and Fisher, J. B.: Global estimates of evapotranspiration
627 for climate studies using multi-sensor remote sensing data: Evaluation of three process-based
628 approaches, Remote Sensing of Environment, 115, 801-823, 2011.
629 Webster, E., Ramp, D., and Kingsford, R. T.: Incorporating an iterative energy restraint for the Surface
630 Energy Balance System (SEBS), Remote Sensing of Environment, 198, 267-285, 2017.
631 Wilson, J. L., and Guan, H.: Mountain-Block Hydrology and Mountain-Front Recharge, in: Groundwater
632 Recharge in a Desert Environment: The Southwestern United States, American Geophysical Union,
633 113-137, 2004.
634 Wilson, K., Goldstein, A., Falge, E., Aubinet, M., Baldocchi, D., Berbigier, P., Bernhofer, C., Ceulemans,
635 R., Dolman, H., and Field, C.: Energy balance closure at FLUXNET sites, Agricultural and Forest
636 Meteorology, 113, 223-243, 2002.
637 Wilson, K. B., Hanson, P. J., Mulholland, P. J., Baldocchi, D. D., and Wullschleger, S. D.: A comparison
638 of methods for determining forest evapotranspiration and its components: sap-flow, soil water
639 budget, eddy covariance and catchment water balance, Agricultural and forest Meteorology, 106, 153-
640 168, 2001.
641 Yang, X., Liu, Q., He, Y., Luo, X., and Zhang, X.: Comparison of daily and sub-daily SWAT models for
642 daily streamflow simulation in the Upper Huai River Basin of China, Stochastic environmental research
643 and risk assessment, 30, 959-972, 2016.
644 Zhang, B., Kang, S., Li, F., and Zhang, L.: Comparison of three evapotranspiration models to Bowen
645 ratio-energy balance method for a vineyard in an arid desert region of northwest China, Agricultural
646 and Forest Meteorology, 148, 1629-1640, 2008a.
647 Zhang, K., Kimball, J. S., and Running, S. W.: A review of remote sensing based actual
648 evapotranspiration estimation, Wiley Interdisciplinary Reviews: Water, 3, 834-853, 2016.

649 Zhang, X., Srinivasan, R., Debele, B., and Hao, F.: Runoff simulation of the headwaters of the Yellow
650 River using the SWAT model with three snowmelt algorithms, JAWRA Journal of the American Water
651 Resources Association, 44, 48-61, 2008b.
652 Zhao, L., Xia, J., Xu, C.-y., Wang, Z., Sobkowiak, L., and Long, C.: Evapotranspiration estimation methods
653 in hydrological models, J. Geogr. Sci, 23, 359-369, 2013.

654

Hydrol. Earth Syst. Sci. Discuss., https://doi.org/10.5194/hess-2017-599
Manuscript under review for journal Hydrol. Earth Syst. Sci.
Discussion started: 24 October 2017

Hydrology and Earth System Sciences
Discussions

Appendix A: Evapotranspiration in SWAT

SWAT provides the user with three options of modelling ET at the HRU level and at daily temporal resolution (Penman-Monteith, Hargreaves or Priestly-Taylor methods). In this study, the Penman-Monteith method is used. SWAT initially calculates the potential evapotranspiration (PET) for a reference crop (Alfalfa) using the Penman-Monteith equation for well-watered plants (Jensen et al., 1990):

$$\lambda E_0 = \frac{\Delta(H_{net}-G)+\rho.c_p.\frac{e_{sat}-e}{r_a}}{\Delta+\gamma(1+\frac{r_c}{r_a})} \quad \text{(A1)}$$

where λ is the latent heat of vaporization (MJ kg^{-1}); E_0 is the potential evapotranspiration rate (mm/d); Δ is the slope of the saturation vapor pressure vs temperature curve (kPa ^{o}C^{-1}); H_{net} is the net radiation at the surface (MJ m^{-2} d^{-1}); G is the heat flux density to the ground (MJ m^{-2} d^{-1}); ρ is the air density (kg m^{-3}); c_p is the specific heat of dry air at constant pressure (J kg^{-1} K^{-1}); P is the atmospheric pressure (kPa); e_{sat} is saturation vapor pressure of air (kPa); e is water vapor pressure (kPa); r_a is the aerodynamic resistance (s m^{-1}); γ is the psychometric constant (kPa ^{o}C^{-1}) and r_c is the canopy resistance (s m^{-1}).

Total ET (AET) in SWAT is made up of four components: canopy evaporation, transpiration, soil evaporation and groundwater ET (Revap). Revap is the movement of water from the saturated zone into the overlying unsaturated zone to supplement the water need for evapotranspiration. The Revap process may be insignificant in regions where the saturated zone is much deeper than the root zone and as such the result is separately reported from the ET result in the SWAT result database. As SWAT calculates Revap separately, for a calculation of AET in regions where the saturated zone is within the root zone, the user should add the Revap result column to the ET calculations. The AET components are calculated from the PET starting with the canopy evaporation. For this first component the following storage equations are used in determining the volume of water available for evaporation from the wet canopy in SWAT

$$C_{day} = C_{mx}\left(\frac{L_{ai}}{L_{ai\_mx}}\right) \quad \text{(A2)}$$

when $R'_{day} \le C_{day} - R_{int(i)}$:

$$R_{int(f)} = R_{int(i)} + R'_{day}\,; and\ R_{day} = 0 \quad \text{(A3)}$$

when $R'_{day} > C_{day} - R_{int(i)}$:

$$R_{int(f)} = C_{day};\ R_{day} = R'_{day} - \left(C_{day} - R_{int(i)}\right) \quad \text{(A4)}$$

where C_{day} is the maximum amount of water that can be stored in the canopy on a given day (mm); C_{mx} is the amount of water that can be stored in the canopy when the canopy is fully matured (mm); L_{ai} is the leaf area index on a given day (); L_{ai_mx} is the maximum leaf area index when the plant is fully matured (-); $R_{int(i)}$ is the initial amount of free water available in the canopy at the beginning of the day (mm); $R_{int(f)}$ is the final amount of free water available in the canopy at the end of the day (mm); R'_{day} is the amount of precipitation on a given day before accounting for canopy interception (mm); and R_{day} is the amount of precipitation reaching the soil on a given day (mm).

The SWAT ET algorithm initially evaporates as much water as can be accommodated in the PET from the wet canopy. If the total volume of water in canopy storage equals or exceeds PET for the day, then ET is calculated as

$$E_a = E_{can} = E_0 \quad \text{(A5)}$$

where E_a is AET (mm d^{-1}); E_{can} is evaporation from canopy constrained by E_0, i.e. PET (mm d^{-1}). However, if the water in canopy storage is less than the PET for the day, transpiration, soil evaporation and Revap are constrained by E'_0, which is the potential evapotranspiration adjusted for the evaporation of the water on the canopy surface (mm d^{-1}).

$$E'_0 = E_0 - E_{can} \quad \text{(A6)}$$

The second AET component (transpiration) of SWAT is calculated using the following equations;

$$\lambda E_{t\_max} = \frac{\Delta(H_{net}-G)+\gamma K(\frac{0.622.\lambda.\rho}{P})\frac{e_{sat}-e}{r_a}}{\Delta+\gamma(1+\frac{r_c}{r_a})} \quad \text{(A7)}$$

$$W_z = \left(\frac{E_{t\_max}}{1-e^{-\tau}}\right) \times \left(1 - e^{(-\tau \times (\frac{z}{zr}))}\right) \quad \text{(A8)}$$

$$W'_l = W_l + (W_d \times e_{pco}) \quad \text{(A9)}$$

$$W"_l = W'_l \times e^{\left(5\times\left(\frac{S_{wl}}{(0.25\times A_{wcl})}-1\right)\right)} \; when \; S_{wl} < 25\% \; of \; A_{wcl} \quad \text{(A10)}$$

$$W"_l = W'_l \; when \; S_{wl} > 25\% \; of \; A_{wcl} \quad \text{(A11)}$$

$$E_{t,l} = \min[W"_l, (S_{wl} - W_{pl})] \quad \text{(A12)}$$

$$E_t = \sum_{l=1}^{n} E_{t,l} \quad \text{(A13)}$$

where E_{t_max} is the maximum transpiration rate (mm/d); $K = 8.64 \times 10^4$; P is the atmospheric pressure (kPa); W_z is the potential water taken up by plant from the soil surface to a specific depth (mm/d) z; τ is the plant water consumption distribution function; z is the depth from soil surface (mm); z_r is the plant root depth from soil

surface (mm); W_l is the potential water consumption by plant in the soil layer l (mm); W'_l is the potential water consumption by plant in the layer l adjusted for demand (mm); W_d is the plant water consumption demand deficit from overlying soil layers (mm); e_{pco} is the plant water consumption compensation factor (-); $W"_l$ is the potential plant water consumption adjusted for initial soil water content (mm); S_{wl} is the soil water content of layer l in a day (mm); A_{wcl} is the available water capacity of layer l (mm); W_{pl} is soil water content of layer l at wilting point (mm); $E_{t,l}$ is the actual transpiration water volume from layer l in a given day (mm/d); E_t is the total actual transpiration by plants in a given day (mm/d). Plant transpiration parameters such as stomatal conductance, maximum leaf area index and maximum plant height are retrieved from a SWAT database while climate data required by the Penman-Monteith method are sourced from input data.

The third AET SWAT component, the soil evaporation on a given day, is a function of the transpiration, degree of shading and potential evapotranspiration adjusted for canopy evaporation. The maximum soil evaporation on a given day (E_s) (mm d^{-1}) is calculated as

$$E_s = E'_0 cov_{sol} \quad \text{(A14)}$$

$$cov_{sol} = e^{(-5.0\ 10^{-5} CV)} \quad \text{(A15)}$$

where cov_{sol} is the soil cover index (-) and CV is the aboveground biomass for the day (kg/ha). The maximum possible soil evaporation in a day is then subsequently adjusted for plant water use (E'_s) (mm d^{-1})

$$E'_s = min\left(E_s, \frac{E_s E'_0}{E_s + E_t}\right) \quad \text{(A16)}$$

The SWAT ET algorithm then partitions the evaporative demand between the soils layers, with the top 10 mm of soil accounting for 50% of soil water evaporated. Equation 17 and 18 are used to calculate the evaporative demand at specific depths and evaporative demands for soil layers respectively.

$$E_{soil,z} = E''_s \frac{z}{z + e^{(2.374 - (0.00713\ z))}} \quad \text{(A17)}$$

$$E_{soil,l} = E_{soil,zl} - E_{soil,zu} \cdot e_{sco} \quad \text{(A18)}$$

$$E'_{soil,l} = E_{soil,l} \times e^{\left(2.5 \times \left(\frac{S_{wl} - F_{cl}}{(F_{cl} - W_{pl})} - 1\right)\right)} \ when\ S_{wl} < F_{cl} \quad \text{(A19)}$$

$$E'_{soil,l} = E_{soil,l}\ when\ S_{wl} > F_{cl} \quad \text{(A20)}$$

$$E"_{soil,l} = \min[E'_{soil,l}, 0.8(S_{wl} - W_{pl})] \quad \text{(A21)}$$

$$E_{soil} = \sum_{l=1}^{n} E"_{soil,l} \quad \text{(A22)}$$

where $E_{soil,z}$ is the water demand for evaporation at depth z (mm); E_s'' is the maximum possible water to be evaporated in a day (mm); e_{sco} is the soil evaporation compensation factor; $E_{soil,l}$ is the water demand for evaporation in layer l (mm); $E_{soil,zl}$ is the evaporative demand at the lower boundary of the soil layer (mm); $E_{soil,zu}$ is the evaporative demand at upper boundary of the soil layer (mm); F_{cl} is the water content of the soil layer l at field capacity (mm) and $E"_{soil,l}$ is the volume of water evaporated from soil layer l (mm/d); E_{soil} is the total volume of water evaporated from soil on a given day (mm/d).

The fourth component of the ET calculations in SWAT is referred to as "Revap". Revap in SWAT is the amount of water transferred from the hydraulically connected shallow aquifer to the unsaturated zone in response to water demand for evapotranspiration. The Revap component in SWAT is akin to ET from groundwater. Revap is often a dominant catchment process in a groundwater dependent ecosystem and it is calculated at the HRU scale. Revap is estimated as a fraction of the potential evapotranspiration (PET) and it is dependent on a threshold depth of water in the shallow aquifer which is set by the user.

$$w_{revap,mx} = \beta_{revap} E_0 \quad \text{(A23)}$$

$$w_{revap} = w_{revap,mx} - a_{thr} \quad if$$

$$a_{thr} < a_{sh} < (a_{thr} + w_{revap,mx}) \quad \text{(A24)}$$

$$w_{revap} = 0 \qquad if\ a_{sh} \leq a_{thr} \quad \text{(A25)}$$

$$w_{revap} = w_{revap,mx} \qquad if\ a_{sh} \geq (a_{thr} + w_{revap,mx}) \quad \text{(A26)}$$

where $w_{revap,mx}$ is the maximum volume of water transferred to the unsaturated zone in response to water shortages for the day (mm); β_{revap} is the Revap coefficient (-); w_{revap} is the actual volume of water transferred to the unsaturated zone to supplement water shortage for the day (mm); a_{sh} is the water volume stored in the shallow aquifer at the beginning of the day (mm); and the a_{thr} is the threshold water level in the shallow aquifer required for Revap to occur (mm) (Neitsch et al., 2011).

Hydrol. Earth Syst. Sci. Discuss., https://doi.org/10.5194/hess-2017-599
Manuscript under review for journal Hydrol. Earth Syst. Sci.
Discussion started: 24 October 2017

Hydrology and Earth System Sciences
Discussions

762 **Appendix B: MODIS Evapotranspiration**

763

764 ET in the MOD16 is a summation of three components: wet canopy evaporation, plant transpiration and soil
765 evaporation. Wet canopy evaporation (λ_{can}) in MOD16 is calculated using a modified version of the Penman-
766 Monteith equation,

767 $$\lambda E_{can} = \frac{(\Delta H_{net}\ F_C)+\rho c_p(e_{sat}-e)\frac{F_{par}}{r_a}F_{wet}}{\Delta+\left(\frac{P\ C_p\ r_{vc}}{\lambda\ \varepsilon\ r_a}\right)} \quad \text{(B1)}$$

768 Where the parameters are as earlier defined, λE_{can} is the latent heat flux (Wm^{-2}); H_{net} is net radiation relative to
769 canopy (Wm^{-2}); F_{par} is the fraction of absorbed photosynthetically active radiation ; F_{wet} is the fraction of the
770 soil covered by water; r_{vc} is the resistance to latent heat transfer (s m^{-1}); and ε is the emissivity.

771

772 The plant transpiration (λE_t) is calculated using another variation of the Penman-Monteith equation,

773 $$\lambda E_t = \frac{(\Delta H_{net}\ F_C)+\rho c_p(e_{sat}-e)\frac{F_C}{r_a}(1-F_{wet})}{\Delta+\gamma\left(1+\frac{r_c}{r_a}\right)} \quad \text{(B2)}$$

774 The soil evaporation (λE_{soil}) is a summation of the potential soil evaporation (λE_{soil_POT}) limited by the soil
775 moisture constraint function (Fisher et al., 2008) and the evaporation from wet soil (λE_{wet_soil}):

776 $$\lambda E_{soil} = \lambda E_{wet\_soil} + \lambda E_{soil\_POT}\left(\frac{R_h}{100}\right)^{\frac{V_{PD}}{\phi}} \quad \text{(B3)}$$

777 $$\lambda E_{wet\_soil} = \frac{(\Delta\ H_{net})+\rho c_p(1.0-F_C)\frac{V_{PD}}{r_a}(F_{wet})}{\Delta+\gamma\left(\frac{r_{tot}}{r_a}\right)} \quad \text{(B4)}$$

778 $$\lambda E_{soil\_POT} = \frac{(\Delta H_{net})+\rho c_p(1.0-F_C)\frac{V_{PD}}{r_a}(1-F_{wet})}{\Delta+\gamma\left(\frac{r_{tot}}{r_a}\right)} \quad \text{(B5)}$$

779 where H_{net} and r_a are relative to the soil surface; r_{tot} is the total aerodynamic resistance to vapor transport (s m^{-1}); V_{PD} is the vapor pressure deficit (Pa); R_h is the relative humidity (%); and β is a dimnesionless coefficient
781 defining the relative sensitivity of R_h to V_{PD}. In MOD16 the constant ϕ is set to 200.

782 Total evapotranspiration (λE) in MOD16 is thus calculated as

783 $$\lambda E = \lambda E_{can} + \lambda E_t + \lambda E_{soil} \quad \text{(B6)}$$

784

785